Field dependence of magnetization reversal by spin transfer

J. Grollier,[1] V. Cros,[1] H. Jaffrès,[1] A. Hamzic,[1,*] J. M. George,[1] G. Faini,[2] J. Ben Youssef,[3] H. Le Gall,[3] and A. Fert[1]
[1]*Unité Mixte de Physique CNRS-THALES and Université Paris-Sud, 91404 Orsay, France*
[2]*Laboratoire de Photonique et de Nanostructures, Route de Nozay, 91460 Marcoussis, France*
[3]*Laboratoire de Magnétisme de Bretagne, Université de Bretagne Occidentale, 29285 Brest, France*
(Received 31 October 2002; published 5 May 2003)

We describe and analyze the effect of an applied field (H_{appl}) on the current-driven magnetization reversal in pillar-shaped Co/Cu/Co trilayers. Depending on the magnitude of H_{appl}, we observe two different types of transitions between the parallel (P) and antiparallel (AP) magnetic configurations of the the Co layers. If H_{appl} is smaller than some threshold value, the transitions between P and AP are relatively sharp and irreversible. For H_{appl} exceeding this threshold value, the transitions are progressive and reversible. We show that this behavior can be precisely accounted for by introducing the current-induced torque of the spin transfer models into a Landau-Lifshitz-Gilbert equation to determine the stability or instability of the P and AP states. This analysis also provides a good description for the field dependence of the critical currents.

DOI: 10.1103/PhysRevB.67.174402 PACS number(s): 75.60.Jk, 75.70.Cn, 73.40.−c

I. INTRODUCTION

In 1996, Slonczewski[1] and Berger[2] predicted that the magnetization of a magnetic layer can be reversed by injection of a spin polarized current and spin transfer to the layer. Magnetization reversal without application of an external magnetic field would be of considerable interest to switch magnetic microdevices, so that these theoretical predictions prompted extensive experimental studies of the effect of spin polarized currents on magnetic nanostructures.[3–12] The most quantitative results have been obtained on multilayered pillars,[7,9–11] typically Co/Cu/Co trilayers, in which the magnetic moment of a thin Co layer is reversed by the spin-polarized current injected from a thicker Co layer. These experiments have confirmed some of the main features predicted by the theory: (i) the effects induced by opposite currents are opposite: if the current of a given sign favors the parallel (P) magnetic configuration of the trilayer, the current of the opposite sign favors the antiparallel (AP) configuration; (ii) the current densities needed to switch such magnetic configuration are of the order of magnitude predicted by theory, i.e., 10^7 A/cm^2. On the other hand, the experimental data have not yet established clearly the variation of the critical currents with the layer thickness, nor has the effect of an applied magnetic field been fully understood.

From the theoretical point of view, several models have been developed. In most of them,[13–20] the calculation of the current-induced torque is based on Slonczewski's concept[1] of spin transfer involving the transverse components of the current spin polarization. Another approach, proposed by Heide,[20] involves the longitudinal components of the polarization and the effect of the current is expressed by an effective exchange-like interaction between the magnetic moments of the two magnetic layers. The second theoretical issue, after calculating the torque, is the description of the reversal process induced by the torque in the presence of applied and anisotropy fields and, in particular, the determination of the critical currents.[4,21–22]

Here we focus on the influence of an applied field H_{appl} on the magnetization reversal induced by a spin current. We will analyze our experimental results on Co/Cu/Co pillars (that were partially published elsewhere[9]) and show the existence of two different field regimes. If the applied field does not exceed some threshold value, there is an irreversible and relatively sharp transition between the parallel (P) and antiparallel (AP) magnetic configurations of the Co layers. In a second regime, for fields above this threshold value, the transition between P and AP is progressive and reversible. We will explain that this behavior can be well accounted for by introducing the current-induced torque of the spin transfer models in a Landau-Lifshitz-Gilbert equation to study the stability of the P and AP states. It will also be shown that the existence of these different regimes of the field dependence of the critical currents cannot be explained in a model describing the effect of the current as an effective exchangelike interaction between the magnetic moments of the cobalt layers.[20] A second important issue—the dependence of the critical currents on the layer thicknesses—will be discussed in a further publication.

In Sec. II, we describe the results we obtain in experiments where the current varies at constant magnetic field. These experiments give clear evidence of two different regimes. In Sec. III, we present our theoretical analysis of the stability of the P and AP configurations and we interpret the experimental results of Sec. II. In Sec. IV, devoted to a different experimental approach for the study the magnetization reversal by spin transfer, we present and discuss experiments in which the field varies at constant current. The field dependence of the critical currents is analyzed in Sec. V and we summarize our conclusions in Sec. VI.

II. RESISTANCE vs CURRENT AT CONSTANT APPLIED MAGNETIC FIELD

Our experiments have been performed on pillar-shaped Co1(15 nm)/Cu(10 nm)/Co2(2.5 nm) trilayers. The submicronic (200×600 nm^2) pillars are fabricated by *e*-beam lithography. Details on the fabrication have been described elsewhere.[9] The trilayer exhibits CPP-GMR effects, with a difference of about 1 mΩ between the resistances in the P

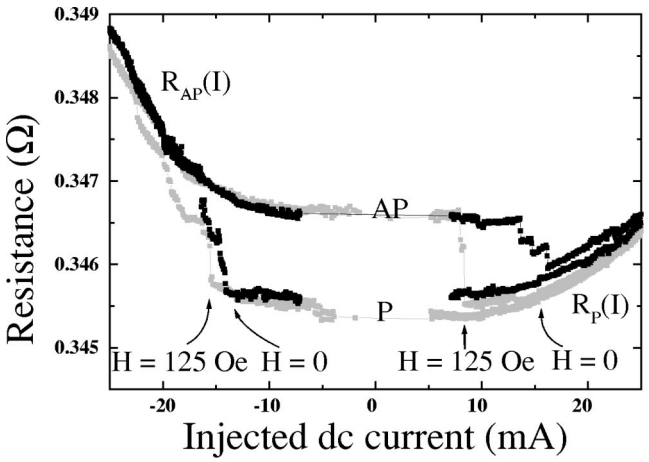

FIG. 1. Resistance vs dc current in sample 1 for $H_{\mathrm{appl}}=0$ (black) and $H_{\mathrm{appl}}=125$ Oe (gray).

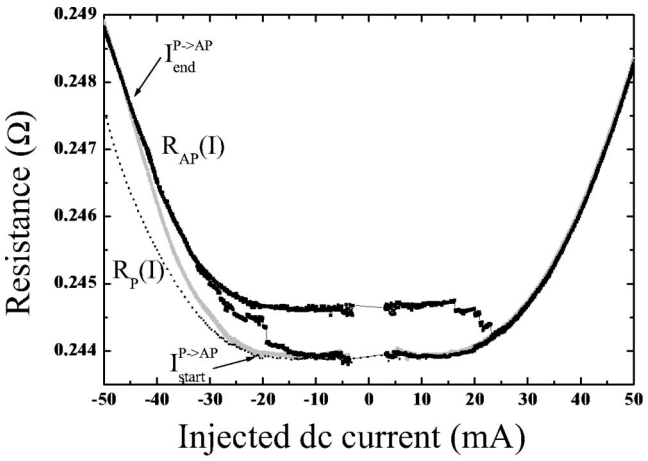

FIG. 2. Resistance vs dc current in sample 2 for $H_{\mathrm{appl}}=0$ (black), $H_{\mathrm{appl}}=+500$ Oe (gray), and $H_{\mathrm{appl}}=+5000$ Oe (dotted line).

and AP configurations. This change of resistance (GMR effect) has been used to determine the changes of the magnetic configuration of the trilayer.

For all the experimental data we present, the initial magnetic configuration (prior to the injection of a dc current) is a parallel (P) magnetic configuration of the system with the magnetic moments of the Co layers along the positive direction of an axis parallel to the long side of the rectangular pillar. The magnetic field H_{appl} is applied along the positive direction of the same axis (thus stabilizing this initial P magnetic configuration). We record the variation of the pillar resistance (R) as the dc current (I) is increased or decreased. The results we report here are obtained at 30 K (the critical currents are smaller at room temperature). In our definition, a positive dc current corresponds to the electron flow from the thick Co layer to the thin one.

In Fig. 1, we present the variation of the resistance R as a function of the dc current I for $H_{\mathrm{appl}}=0$ and 125 Oe. Starting from a P configuration (for $I=0$) and increasing the current to positive values, we observe only a progressive and reversible small increase of the resistance R, which can be ascribed to some heating of the sample (this has been also seen in all other experiments on pillars[7,9–11] when the current density reaches the range of 10^7 A/cm^2). In contrast, when the current is negative and at a critical value $I_C^{\mathrm{P}\to\mathrm{AP}}$, an irreversible jump of the resistance ($\Delta R\approx 1\ \mathrm{m}\Omega$) is clearly seen, which corresponds to a transition from the P to the AP configurations and therefore indicates the reversal of the magnetic moment of the thin Co layer. The trilayer then remains in this high resistance state [the $R_{\mathrm{AP}}(I)$ curve] until the current is swept to positive values, where, at the critical current $I_C^{\mathrm{AP}\to\mathrm{P}}$, the resistance drops back to the $R_P(I)$ curve. In a small range of applied magnetic field (that we shall note as *regime A*), this type of hysteretic $R(I)$ curve is the fingerprint of the magnetization reversal by spin injection.[7,9–11]

If the applied magnetic field is zero, $I_C^{\mathrm{P}\to\mathrm{AP}}\cong -15$ mA (corresponding to the current density $j_C^{\mathrm{P}\to\mathrm{AP}}\cong -1.25\times 10^7$ A/cm^2) and $I_C^{\mathrm{AP}\to\mathrm{P}}\cong +14$ mA ($j_C^{\mathrm{AP}\to\mathrm{P}}\cong +1.17\times 10^7$ A/cm^2). With a positive applied field, which stabilizes the P configuration, $|I_C^{\mathrm{P}\to\mathrm{AP}}|$ increases and $I_C^{\mathrm{AP}\to\mathrm{P}}$ decreases. This is seen in Fig. 1 by comparing the critical currents values obtained for $H_{\mathrm{appl}}=0$ and $H_{\mathrm{appl}}=+125$ Oe. We, however, emphasize that, in this example, the shift of $I_C^{\mathrm{AP}\to\mathrm{P}}$, induced by the applied field, is larger than that of $I_C^{\mathrm{AP}\to\mathrm{P}}$.

The $R(I)$ curve for $H_{\mathrm{appl}}=+500$ Oe (shown in Fig. 2) illustrates the different behavior we observe when the applied fields are higher (which we call *regime B*). Starting from $I=0$ in a P configuration [on the $R_{\mathrm{P}}(I)$ curve], a large enough negative current still induces a transition from P to AP, but now this transition is very progressive and reversible. The $R(I)$ curve departs from the $R_{\mathrm{P}}(I)$ curve at $I_{\mathrm{start}}^{\mathrm{P}\to\mathrm{AP}}\cong -25$ mA ($j_{\mathrm{start}}^{\mathrm{P}\to\mathrm{AP}}\cong -2.08\times 10^7$ A/cm^2), reaches finally $R_{\mathrm{AP}}(I)$ at $I_{\mathrm{end}}^{\mathrm{P}\to\mathrm{AP}}\cong -45$ mA ($j_{\mathrm{end}}^{\mathrm{P}\to\mathrm{AP}}\cong -3.75\times 10^7$ A/cm^2) and, for higher negative values of the current, the resistance continues to follow the $R_{\mathrm{AP}}(I)$ curve. On the way back (towards positive values of the current), $R(I)$ departs from $R_{\mathrm{AP}}(I)$ at $I_{\mathrm{start}}^{\mathrm{AP}\to\mathrm{P}}=I_{\mathrm{end}}^{\mathrm{P}\to\mathrm{AP}}\cong -45$ mA and reaches finally $R_{\mathrm{P}}(I)$ at $I_{\mathrm{end}}^{\mathrm{AP}\to\mathrm{P}}=I_{\mathrm{start}}^{\mathrm{P}\to\mathrm{AP}}\cong -25$ mA. If the same type of experiment is done at even higher values of the applied field, the transition is similarly progressive and reversible, but occurs in a higher negative current range. Finally, for very large applied field ($H_{\mathrm{appl}}=5000$ Oe), the transition is out of our experimental current range, and the recorded curve is simply $R_{\mathrm{P}}(I)$.

III. CALCULATION OF THE CRITICAL CURRENTS IN THE PRESENCE OF AN EXTERNAL FIELD

In order to study the stability or instability of a P (AP) configuration in the presence of a dc current, we will study the motion of the magnetic moment of the thin cobalt layer by using a Landau-Lifshitz-Gilbert (LLG) equation in which we introduce a current-induced torque of the form predicted by Slonczewski.[1] This approach is certainly less quantitatively precise than those based on micromagnetics simulations with non-uniform magnetization,[22] but, as we will see, it can nevertheless account for most of the qualitative features of the experimental results.

Our notation is summarized in Fig. 3. We denote the unit

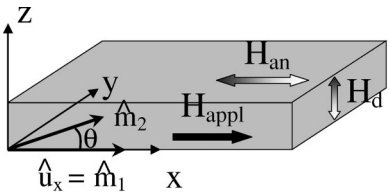

FIG. 3. Notation for the calculation of Sec. III: $\hat{m}_1$ and $\hat{m}_2$ are unit vectors along the magnetization of the thick and thin magnetic layers respectively; there is an uniaxial magnetic anisotropy field H_{an} along the x axis (long side of the rectangular layers in our experiments); $\hat{m}_1$ and the applied field H_{appl} are in the positive direction of the x axis.

vectors along the magnetic moments of the thick and thin Co layers as $\hat{m}_1$ and $\hat{m}_2$, respectively. We suppose that there is an uniaxial magnetic anisotropy in the layer plane along the x axis (the long side of the rectangular layers in our experiments) and that $\hat{m}_1$ is fixed in the positive direction of this axis. We note $\hat{u}_x \equiv \hat{m}_1$ the unit vector along the x axis, and $\hat{u}_z$ the unit vector along the z axis perpendicular to the layers. The magnetic field H_{appl}, as in our experiments, is applied along the x axis. The stability conditions for the P or AP configurations are obtained by studying the motion of $\hat{m}_2$ when the angle θ between $\hat{m}_2$ and $\hat{u}_x$ is close to either 0 or π. The LLG equation can be written as

$$\frac{d\hat{m}_2}{dt} = -\gamma_0 \hat{m}_2 \times [H_{\text{eff}} \hat{u}_x - H_d (\hat{m}_2 . \hat{u}_z) \hat{u}_z] + \alpha \hat{m}_2 \times \frac{d\hat{m}_2}{dt} - G^{\text{P(AP)}} j \hat{m}_2 \times (\hat{m}_2 \times \hat{u}_x), \quad (1)$$

where

$$H_{\text{eff}} = H_{\text{appl}} \pm H_{\text{an}}. \quad (2)$$

$H_d = 4\pi M_s$ describes the anisotropy induced by the demagnetizing field, H_{an} is the in-plane uniaxial anisotropy, + or − depend whether the configuration is close to P or AP, and α is the Gilbert damping coefficient. The last term in Eq. (1) is the contribution from the spin torque,[1] j is the current density and

$$G^{\text{P(AP)}} = \frac{2\mu_B P_S^{\text{P(AP)}}}{t_2 M_s e}. \quad (3)$$

The coefficient P_S is a coefficient of transverse spin polarization and takes different value (P^{P} or P^{AP}) depending on whether $\hat{m}_2$ is close to either the P or the AP configuration, t_2 is the thickness of the thin Co layer and M_s is the Co magnetization.

At this point, it could be noted that an analytical approach based on equations similar to Eq. (1) has already been used by Katine *et al.*[7] and Sun[21] to derive the critical currents. However, these authors have considered a particular case only. They first solved the LLG equation without the Gilbert and current-induced terms and derived the motion equation for the small periodic elliptical precession of $\hat{m}_2$ around $\hat{u}_x$ (or $-\hat{u}_x$) generated by only the field terms of Eq. (1). They then calculated the work of the Gilbert and current-induced terms of Eq. (1) (during a period of this elliptical precession), and derived the stability or instability of the configuration from the sign of the calculated work. This method can be applied only when the motion generated by the applied, anisotropy and demagnetizing field, is a periodic precession, i.e., for $H_{\text{appl}} < H_{\text{an}}$ (when $\hat{m}_2$ is close to $-\hat{u}_x$ around the AP configuration) and for $H_{\text{appl}} > -H_{\text{an}}$ (when $\hat{m}_2$ is close to $+\hat{u}_x$ around the P configuration). Our present calculation is more general and holds for any value of the applied field as long as it is smaller than the demagnetizing field. As a consequence, we will show that the *regime B* of our experimental results is expected in a field range where the approach of Katine *et al.*[7] and Sun[21] cannot be applied.

Projecting the LLG equations onto the three axes x, y, and z, we obtain the following equations for the components m_x, m_y, and m_z of $\hat{m}_2$:

$$\begin{aligned} \dot{m}_x &= \gamma_0 H_d m_z m_y + \alpha m_y \dot{m}_z - \alpha m_z \dot{m}_y + G^{\text{P(AP)}} j (m_y^2 + m_z^2), \\ \dot{m}_y &= -\gamma_0 H_{\text{eff}} m_z - \gamma_0 H_d m_z m_x + \alpha m_z \dot{m}_x - \alpha m_x \dot{m}_z \\ &\quad - G^{\text{P(AP)}} j m_x m_y, \\ \dot{m}_z &= \gamma_0 H_{\text{eff}} m_y + \alpha m_x \dot{m}_y - \alpha m_y \dot{m}_x - G^{\text{P(AP)}} j m_x m_z. \end{aligned} \quad (4)$$

When the angle θ between $\hat{m}_2$ and $\hat{u}_x = \hat{m}_1$ is small (or close to π), by keeping only the terms of first order in m_y and m_z and also neglecting the terms in α^2 (the Gilbert coefficient is a small number), Eq. (4) can be written as

$$\begin{aligned} m_x &= \pm 1, \\ \dot{m}_y &= \mp(\alpha\gamma_0 H_{\text{eff}} + Gj) m_y + [-\gamma_0 (H_{\text{eff}} \pm H_d) + \alpha G j] m_z, \\ \dot{m}_z &= (\gamma_0 H_{\text{eff}} - Gj) m_y + [-\alpha\gamma_0 (\pm H_{\text{eff}} + H_d) \mp \alpha G j] m_z, \end{aligned} \quad (5)$$

where $\pm$ ($\mp$) means + (−) when the configuration is close to P, and − (+) when the configuration is close to AP. Also, G is G^{P} or G^{AP}. The general solutions for m_y and m_z are of the form

$$A \exp(k_1 t) + B \exp(k_2 t). \quad (6)$$

The condition for the instability of a given magnetic configuration (P or AP) is related to the sign of the real part of k_1 and k_2: a positive sign means that the amplitude of the motion of $\hat{m}_2$ increases with time and that the configuration is unstable. k_1 and k_2 are the solutions of the quadratic equation which, after dropping the terms of second order in α, is written as

$$k^2 \pm 2k \left[2\gamma_0 \left(H_{\text{eff}} \pm \frac{H_d}{2} \right) \pm Gj \right] + G^2 j^2 + \gamma_0^2 H_{\text{eff}} (H_{\text{eff}} \pm H_d) = 0. \quad (7)$$

The solution of Eq. (7) and the expressions for k_1 and k_2 are detailed in Appendix A. Here, we focus on the results corresponding to our experiments, i.e., when H_{appl} is positive and thus favors the orientation of $\hat{m}_2$ (thin layer) in the direction parallel to $\hat{u}_x = \hat{m}_1$ (thick layer). The results for nega-

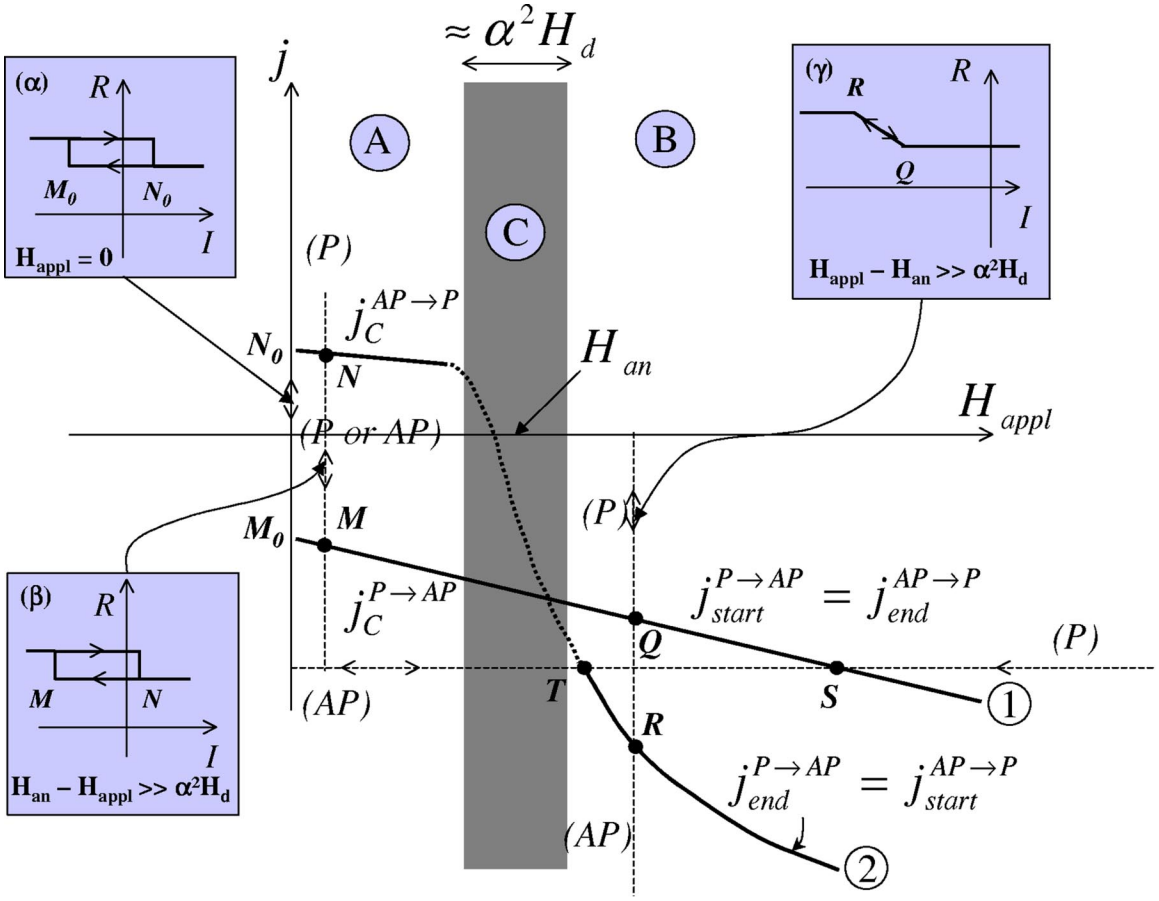

FIG. 4. Critical currents vs applied field (schematic representation). The line 1, derived from Eq. (8) ≡ Eq. (10), separates the regions where the P configuration is stable (above the line) and unstable (below). The line 2, derived from Eq. (9) in *regime A* and Eq. (11) in *regime B*, separates the regions where the AP configuration is stable (below the line) and unstable (above). The dotted curve in the zone $\approx \alpha^2 H_d$ is a guide for the eye in the cross over regime between *regime A* and *B*. In *regime A*, the stability regions of P and AP overlap between the curves 1 and 2, which leads to the hysteretic behavior shown in insets (α) and (β), see discussion in the text. In *regime B*, the P and AP configurations are both unstable in the region between curves 1 and 2, which leads to the progressive and reversible transition shown in inset (γ), see text.

tive values of H_{appl} are presented in Appendix B.

The overall behavior for $H_{\mathrm{appl}}>0$ can be separated into three different regimes, which we will now discuss separately. They are also schematically depicted in Fig. 4.

A. $H_{\mathrm{appl}}>0$ and $H_{\mathrm{an}}-H_{\mathrm{appl}}\gg\alpha^2 H_d$

This low field regime *A* is for H_{appl} between zero and a few tens of Oe below H_{an} [if one estimates $\alpha^2 H_d$ from the value of α derived from FMR (Ref. 23)]. The P configuration becomes unstable when the sign of the real part of k_1 and k_2 is positive, that is, for

$$j<-\frac{\alpha\gamma_0}{G^{\mathrm{P}}}\left(H_{\mathrm{appl}}+H_{\mathrm{an}}+\frac{H_d}{2}\right),$$

whereas the AP configuration is unstable for

$$j>+\frac{\alpha\gamma_0}{G^{\mathrm{AP}}}\left(-H_{\mathrm{appl}}+H_{\mathrm{an}}+\frac{H_d}{2}\right).$$

It turns out that, in regime *A*, the P and AP configurations are both stable between the negative and positive threshold currents of the two preceding equations. In the diagram of Fig. 4, this corresponds to the overlap of the stability regions of the P and AP configurations between lines 1 and 2 in zone *A*. Thus, starting from a P configuration at zero current and going down to negative values of the current, the P configuration becomes unstable at a current for which the AP configuration is stable, and the system can switch directly from P to AP. This occurs at the critical current density $j_C^{\mathrm{P}\to\mathrm{AP}}$:

$$j_c^{\mathrm{P}\to\mathrm{AP}}=-\frac{\alpha\gamma_0}{G^{\mathrm{P}}}\left(H_{\mathrm{appl}}+H_{\mathrm{an}}+\frac{H_d}{2}\right). \tag{8}$$

In Fig. 4 and in the insets (α) or (β) of Fig. 4, this corresponds to the points M_0 (at zero field) or M (nonzero field). When the current returns to zero and becomes positive, the AP configuration becomes unstable, and it can switch directly to a stable P configuration at the critical current density $j_c^{\mathrm{AP}\to\mathrm{P}}$ [points N_0 and N in Fig. 4 and in the insets (α) and (β) of Fig. 4]:

$$j_c^{\mathrm{AP}\to\mathrm{P}} = +\frac{\alpha\gamma_0}{G^{\mathrm{AP}}}\left(-H_{\mathrm{appl}}+H_{\mathrm{an}}+\frac{H_d}{2}\right). \tag{9}$$

Such a hysteretic behavior, with direct transitions between P and AP, corresponds to our experimental observations at low field (see Fig. 1). A similar behavior and similar equations for the critical currents are obtained in the approach of Katine *et al.*[7] and Sun.[21]

B. $H_{\mathrm{appl}}>0$ and $H_{\mathrm{appl}}-H_{\mathrm{an}}\gg\alpha^2 H_d$

The condition of instability of the P configuration (positive signs of k_1 and k_2) is similar to the one derived for the case *A*, i.e.,

$$j<-\frac{\alpha\gamma_0}{G^{\mathrm{P}}}\left(H_{\mathrm{appl}}+H_{\mathrm{an}}+\frac{H_d}{2}\right).$$

On the other hand, the condition for an unstable AP configuration has changed and becomes

$$j>-\frac{\gamma_0}{G^{\mathrm{AP}}}\left[(H_{\mathrm{appl}}-H_{\mathrm{an}})\left(H_{\mathrm{appl}}-H_{\mathrm{an}}+\frac{H_d}{2}\right)\right]^{1/2}$$

Now there is a current range where none of the P and AP configurations is stable (as this can be shown straightforwardly by comparing the two preceding treshold currents for $(H_{\mathrm{appl}}-H_{\mathrm{an}})\gg\alpha^2 H_d$ and $H_d\gg H_{\mathrm{an}}$). Starting from a P configuration at zero current and sweeping the current to negative values, the P configuration becomes unstable at the critical current density $j_{\mathrm{start}}^{P\to\mathrm{AP}}$ [point *Q* in Fig. 4 and in the inset (γ) of Fig. 4]:

$$j_{\mathrm{start}}^{\mathrm{P}\to\mathrm{AP}} = -\frac{\alpha\gamma_0}{G_{\mathrm{P}}}\left(H_{\mathrm{appl}}+H_{\mathrm{an}}+\frac{H_d}{2}\right). \tag{10}$$

However, the AP configuration is not stable at this current density. Taking into account the condition for the stability around $\theta=\pi$, the AP configuration is reached only at the critical current density $j_{\mathrm{end}}^{\mathrm{P}\to\mathrm{AP}}$ [point *R* in Fig. 4 and in inset (γ) of Fig. 4]:

$$j_{\mathrm{end}}^{\mathrm{P}\to\mathrm{AP}} = -\frac{\gamma_0}{G^{\mathrm{AP}}}[(H_{\mathrm{appl}}-H_{\mathrm{an}})(H_{\mathrm{appl}}-H_{\mathrm{an}}+H_d)]^{1/2}. \tag{11}$$

When the current is swept back, the AP configuration becomes unstable at the same critical current density [see Eq. (11), and point *R* in Fig. 4 and in inset (γ) of Fig. 4]:

$$j_{\mathrm{start}}^{\mathrm{AP}\to\mathrm{P}} = j_{\mathrm{end}}^{\mathrm{P}\to\mathrm{AP}}. \tag{12}$$

The P configuration is reached only for

$$j_{\mathrm{end}}^{\mathrm{AP}\to\mathrm{P}} = j_{\mathrm{start}}^{\mathrm{P}\to\mathrm{AP}} \tag{13}$$

which is the point *Q* in Fig. 4 and in inset (γ) of Fig. 4. We therefore expect a *progressive* and *reversible* transition between P and AP. During the progressive transition, the system is in a state of maintained precession.

C. $H_{\mathrm{appl}}>0$ and $H_{\mathrm{appl}}-H_{\mathrm{an}}\approx\alpha^2 H_d$

The condition for an unstable P configuration is the same as in case *A* or *B*. On the other hand, when θ is close to π, there is no simple analytical solution of Eq. (5) if H_{appl} is in a zone of width $\approx\alpha^2 H_d$ around H_{an} (see Fig. 4). The dotted line in Fig. 4 is what is qualitatively expected for the variation of the critical current of the AP configuration in the crossover zone.

The insets of Fig. 4 summarize the expected $R(I)$ variations. The insets (α) and (β) represent the expected $R(I)$ variations in the *regime A*. The hysteretic behavior is comparable to what is observed experimentally at low field (Fig. 1). In Eqs. (8), (9) for $H_{\mathrm{appl}}=0$, the asymmetry between the critical currents of the P→AP and AP→P transitions in inset (α), comes from the difference between G^{P} and G^{AP}. When H_{appl} increases both transitions are shifted to the left, as represented in inset (β). The larger shift we observe for $j_c^{\mathrm{AP}-\mathrm{P}}$ in Fig. 1 is probably due to the deviations from Eq. (9) when one approaches the crossover region between *regimes A* and *B*. The inset (γ) represents the $R(I)$ curve expected in the *regime B*. The slope corresponds to the progressive and reversible transition between *Q* and *R* in Fig. 4. This behavior corresponds to what is observed experimentally at high field in Fig. 2. Such a behavior cannot be predicted by calculations[7,21] assuming that the motion of $\hat{m}_2$ is a periodic precession, which is obviously not the case in *regime B*.

In order to extend our approach to a more quantitative level, we have also calculated the critical currents in both regimes predicted by Eqs. (8)–(11). The parameter we use are $t_2=2.5$ nm, $P^{\mathrm{P}}=0.07$ and $P^{\mathrm{AP}}=0.41$ (derived in the model of Fert *et al.*[19] from CPP-GMR data on Co/Cu multilayers[24,25]), $\alpha=0.007$ (Ref. 23), $H_d=1.79$ T and $H_{\mathrm{an}}=150$ Oe, which is approximately the field of the crossover between *regimes A* and *B* in our experiments (this value is also close to the value of H_{an} derived from the numerical calculations of Chen *et al.*[26] for rectangular prisms).

For sample 2, in *regime A* and in zero applied magnetic field, we obtain $j_c^{\mathrm{P}\to\mathrm{AP}}=-4.9\times10^7$ A/cm^2 (experimentally, -1.6×10^7 A/cm^2) and $j_c^{\mathrm{AP}\to\mathrm{P}}=+0.8\times10^7$ A/cm^2 (exp., $+1.17\times10^7$ A/cm^2). For $H_{\mathrm{appl}}=500$ Oe in the regime *B*, we obtain $j_{\mathrm{start}}^{\mathrm{P}\to\mathrm{AP}}=-5.1\times10^7$ A/cm^2 (exp., -2.08×10^7 A/cm^2) and $j_{\mathrm{end}}^{\mathrm{P}\to\mathrm{AP}}=-33\times10^7$ A/cm^2 (exp., -3.75×10^7 A/cm^2). This shows that the expressions of the spin transfer model predict the right order of magnitude for the critical currents in both the *A* and *B regimes*. The stronger discrepancy for $j_{\mathrm{end}}^{\mathrm{P}\to\mathrm{AP}}$ may be due to the difficulty to determine precisely the point where the $R(I)$ curve merges into the $R_{\mathrm{AP}}(I)$ curve (see Fig. 2) and to the probable underestimate of $j_{\mathrm{end}}^{\mathrm{P}\to\mathrm{AP}}$.

Finally, it is interesting to see what are the conditions for the occurrence of the instabilities if the effect of the current is described by an effective interaction energy of the form $E_{\mathrm{int}}=-gj\hat{m}_1.\hat{m}_2$, as in the model proposed by Heide.[20] This interaction can be expressed by an effective field $\propto gj\hat{u}_x$ which adds to $H_{\mathrm{eff}}\hat{u}_x$ in the first term of the LLG equation [see Eq. (1)]. Following the same approach as above to determine the stability (or instability) of the P and AP configurations, one can find only a hysteretic behavior with direct transitions for

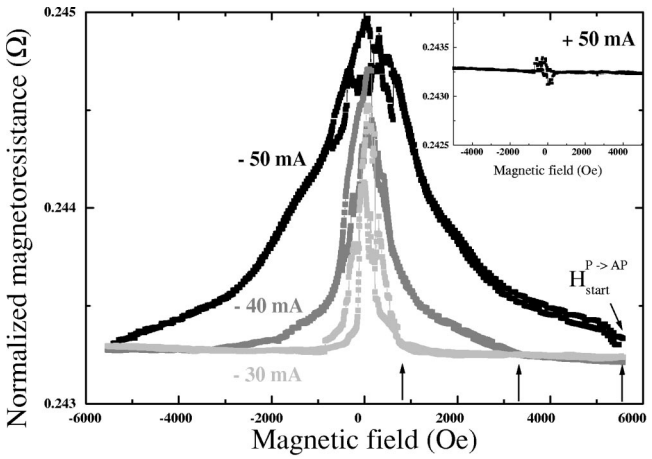

FIG. 5. Resistance vs applied magnetic field in sample 2 for $I=-50$ mA (black), -40 mA (gray), and -30 mA (light gray). For clarity, the curves have been shifted vertically to have the same high field baseline. $R(H)$ for $I=+50$ mA is shown in the inset.

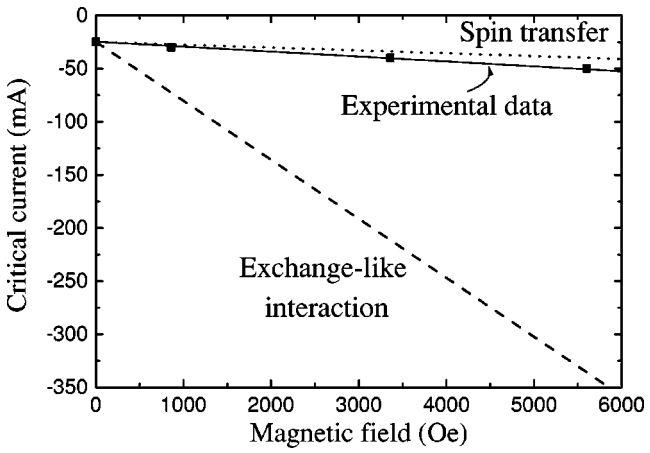

FIG. 6. Field dependence of the critical current for the instability of the P configuration ($j_c^{P\to AP}$ in *regime A* and $j_{start}^{P\to AP}$ in *regime B*). The symbols represent the experimental data for sample 2. The dotted line, from Eq. (15), is the expected variation in spin transfer models based on torques of Slonczewski type. The dashed line, from Eq. (14), is the expected variation for an exchangelike current-induced interaction (Ref. 20).

$$j_c^{P\to AP} = -\gamma_0(H_{appl}+H_{an})/g$$

$$j_c^{AP\to AP} = \gamma_0(H_{an}-H_{appl})/g. \qquad (14)$$

In other words, this approach does not predict the existence of a regime with nonhysteretic and reversible reversal, which is in clear contradiction with the observations at high field. Furthermore, (as we will also show later) the field dependence of the critical currents expected from Eq. (14) is not consistent with the experimental variation. However we cannot rule out some mixing of a small exchange like interaction into a predominant Slonczewski-like term.

IV. RESISTANCE vs APPLIED MAGNETIC FIELD AT CONSTANT dc CURRENT

In Fig. 5, we present the variation of the resistance (R) of a pillar as a function of the applied field (H_{appl}) for several values of the dc currents ($I=+50$, -30, -40, and -50 mA).

The $R(H_{appl})$ curve for $I=+50$ mA is flat, i.e., there is no GMR. This means that a large positive current is able to maintain the P configuration of the Co magnetic moments throughout our experimental field range. This can be compared with what occurs when there is a strong ferromagnetic interlayer coupling.

In negative currents, on the other hand, the $R(H_{appl})$ curves exhibit a bell-shaped profile, which mimics the GMR of an antiferromagnetically coupled trilayer. In addition the width of the bell-shaped $R(H_{appl})$ curves broadens when the current increases, in the same way the GMR curves broaden when the strength of the AF coupling increases. The variation of R with H can be related to what is expected when one moves on the horizontal line ST of the diagram of Fig. 4. Starting from high field at $I=-50$ mA, for example, the upturn from the baseline at about $H_{appl}=+5600$ Oe indicates the beginning of the progressive transition from P to AP at point S in Fig. 4 (in the *regime B* of the diagram, as expected at high field). As H_{appl} decreases from 5600 Oe to a small value close to the anisotropy field, the progressive (and reversible) increase of R corresponds to the progressive crossover from P to AP between S and T. It, however, turns out the noise in the $R(H)$ curves at small field in Fig. 5 does not allow us to determine precisely the field H_T at which the point T is reached. When H_{appl} becomes negative, the moment m_1 of the thick Co layer is reversed. But, at low field (*regime A*) in the presence of a large negative current, the P configuration is unstable and the AP one is stable, so that there is an immediate reversal of m_2 restoring the AP configuration. This explains why there is practically no discontinuity of the $R(H_{appl})$ curves in the region of their maximum.

Quantitative values of $j_{start}^{P\to AP}$ for a given applied field can be extracted from the $R(H_{appl})$ curves, for example, $j_{start}^{P\to AP}(5600\text{ Oe})=-50$ mA. We will make use of these data in the discussion of the field dependence of the critical current of the transition from P to AP in the next section. On the other hand, as discussed above, the value of the field H_T cannot be precisely derived from our experiments, so that $j_{start}^{AP\to P}(H_{appl})$ cannot be reliably estimated and its field dependence will not be discussed.

V. FIELD DEPENDENCE OF THE CRITICAL CURRENTS

The experimental values of the critical current characterizing the instability of the P configuration in one of our samples are plotted as a function of the applied field in Fig. 6. This includes the critical current $j_c^{P\to AP}$ derived from the experiments of Sec. II (for clarity, as the field range of these experiments is very narrow compared to the scale of Fig. 6, only the value at zero field has been plotted) and the critical current $j_{start}^{P\to AP}$ of *regime B* taken from the $R(H_{appl})$ data of Fig. 5. It can be seen that all the experimental points are approximately on the same straight line.

According to Eq. (8) for $j_c^{P\to AP}$ of *regime A* and Eq. (10) for $j_{start}^{P\to AP}$ of *regime B*,

$$j_c^{P\to AP}=j_{start}^{P\to AP}=j_c^{P\to AP}(H_{appl}=0)\left[1+\frac{H_{appl}}{H_{an}+H_d/2}\right]. \tag{15}$$

The variation with H_{appl} calculated with $H_d=1.79$ T and $H_{an}=150$ Oe (see Sec. III) is represented as a dotted line on Fig. 6. The agreement between the slopes of the experimental and calculated lines is rather satisfactory. In contrast the experimental variation is in strong disagreement with the dashed line expected from Eq. (14) when the effect of the current is described by an effective interaction[21] $\propto \hat{m}_1\cdot\hat{m}_2$.

VI. CONCLUSIONS

The following main conclusions can be derived from our experimental results and their analysis.

(1) The experimental results for magnetization reversal by spin transfer in the presence of an external magnetic field show the existence of two qualitatively different regimes: a *low field regime A*, with direct and irreversible transitions between the P and AP configurations of the trilayer, and a *high field regime B* with progressive and reversible transitions. The stage of progressive transition in *regime B* is supposed to be a state with current-maintained precession and spin wave emission.[3,11]

(2) The existence of the *regimes A* and *B* can be theoretically explained by a calculation in which Slonczewski's spin torque is introduced in a LLG equation to study the stability of the P and AP configurations. Our experimental results can be accounted for in the schematic diagram of Fig. 4.

(3) The field dependence of the critical currents can be reasonably well accounted for by the expressions derived by including the spin torque of Slonczewski into the LLG equation. In contrast there is a strong discrepancy between the experimental field dependence and what is expected when the effect of the current is expressed by an effective exchangelike interaction.

ACKNOWLEDGMENTS

This work was supported by the EU through the RTN ''Computational Magnetoelectronics'' (Grant No. HPRN-CT-2000-00143) and the NanoPTT Growth Program (Grant No. GR5D-1999-0135) and also by the Ministère de la Recherche et de la Technologie through the MRT ''Magmem II'' (Grant No. 01V0030) and the ACI contract ''BASIC'' (27-01).

APPENDIX A: INSTABILITY CONDITIONS

When the trilayer is close to the P configuration (θ close to zero), the determinant of Eq. (7) is

$$\Delta=2\alpha\gamma_0 G^P j\left(H_{appl}+H_{an}+\frac{H_d}{2}\right)-\gamma_0^2(H_{appl}+H_{an})(H_{appl}+H_{an}+H_d). \tag{A1}$$

A straightforward numerical estimate shows that, for $H_{appl}>0$ and even for current densities largely exceeding the experimental range Δ is negative. Consequently,

$$k_1=-G^P j-\alpha\gamma_0\left(H_{appl}+H_{an}+\frac{H_d}{2}\right)+i\sqrt{(-\Delta)},$$

$$k_2=-G^P j-\alpha\gamma_0\left(H_{appl}+H_{an}+\frac{H_d}{2}\right)-i\sqrt{(-\Delta)}. \tag{A2}$$

The ellipsoidal magnetization precession around the x axis is related to the imaginary part of k_1 and k_2. On the other hand, the stability of the P state depends on the sign of the real part of k_1 and k_2. For $j<-(\alpha\gamma_0/G^P)(H_{appl}+H_{an}+H_d/2)$, the real parts of k_1 and k_2 are positive, $\exp(k_1 t)$ and $\exp(k_2 t)$ increase with time, which means that the P state is unstable.

The same approach can be applied to discuss the stability of the AP configuration, but the problem is more complex. The determinant is now

$$\Delta=-2\alpha\gamma_0 G^{AP} j\left(-H_{appl}+H_{an}+\frac{H_d}{2}\right)+\gamma_0^2(H_{appl}-H_{an})(-H_{appl}+H_{an}+H_d). \tag{A3}$$

For $H_{appl}>0$ and $H_{an}-H_{appl}\gg\alpha^2 H_d$, the first term in Δ can be neglected and $\Delta=\gamma_0^2(H_{appl}-H_{an})(-H_{appl}+H_{an}+H_d)$ is negative. Thus,

$$k_1=G^{AP} j-\alpha\gamma_0\left(-H_{appl}+H_{an}+\frac{H_d}{2}\right)-i\sqrt{|\Delta|},$$

$$k_2=G^{AP} j-\alpha\gamma_0\left(-H_{appl}+H_{an}+\frac{H_d}{2}\right)+i\sqrt{|\Delta|}. \tag{A4}$$

The real parts of k_1 and k_2 are positive and the AP configuration is unstable for

$$j>\frac{\alpha\gamma_0}{G^{AP}}\left(\frac{H_d}{2}-H_{appl}+H_{an}\right) \tag{A5}$$

For $H_{appl}>0$ and $H_{appl}-H_{an}\gg\alpha^2 H_d$, the first term in Δ can be neglected as well. Δ is positive and

$$k_1=G^{AP} j-\alpha\gamma_0\left(-H_{appl}+H_{an}+\frac{H_d}{2}\right)-\sqrt{\Delta},$$

$$k_2=G^{AP} j-\alpha\gamma_0\left(-H_{appl}+H_{an}+\frac{H_d}{2}\right)+\sqrt{\Delta}. \tag{A6}$$

With $\sqrt{\Delta}\gg\alpha\gamma_0(-H_{appl}+H_{an}+H_d/2)$, the AP state is unstable if k_1 or k_2 is positive. This leads to the condition for the instability of the AP state

$$j>-\frac{\gamma_0}{G^{AP}}\sqrt{(H_{appl}-H_{an})(H_d-H_{appl}+H_{an})}. \tag{A7}$$

APPENDIX B: EXTENSION TO NEGATIVE APPLIED FIELDS

The calculations in the body of the article and in Appendix A have been limited to the situation where both the magnetization of the thick layer and the applied field were in the same positive direction of the x axis (as in our experiments). Now we suppose we reverse the applied field and we look for the extension of the diagram to the left of Fig. 4. We will consider two situations.

(a) In a negative field, the magnetization of the thick layer is reversed $\hat{m}_1 = -\hat{u}_x$ (this is the situation when the applied field exceeds the coercive field of the thick layer).

(b) The magnetization of the thick layer is still positive $\hat{m}_1 = +\hat{u}_x$ (this occurs if, for example, this magnetization is pinned by an antiferromagnetic layer, or this describes also the situation for an applied field smaller than the coercive field of the thick layer).

Calculations similar to those for positive fields lead to the following equations for the critical lines in the extension of the diagram of Fig. 4. In case (a) the expressions of the critical currents are simply obtained from those for $H_{\mathrm{appl}} > 0$ by replacing H_{appl} by $|H_{\mathrm{appl}}|$.

Case (a), *regime A* ($H_{\mathrm{appl}} < 0, H_{\mathrm{an}} - |H_{\mathrm{appl}}| \gg \alpha^2 H_d$): direct and irreversible transitions between P and AP are expected at the critical currents

$$j_c^{\mathrm{P}\to\mathrm{AP}} = -\frac{\alpha\gamma_0}{G^{\mathrm{P}}}\left(|H_{\mathrm{appl}}| + H_{\mathrm{an}} + \frac{H_d}{2}\right)$$

$$j_c^{\mathrm{AP}\to\mathrm{P}} = +\frac{\alpha\gamma_0}{G^{\mathrm{AP}}}\left(-|H_{\mathrm{appl}}| + H_{\mathrm{an}} + \frac{H_d}{2}\right). \qquad \text{(B1)}$$

Case (a), *regime B* ($H_{\mathrm{appl}} < 0, |H_{\mathrm{appl}}| - H_{\mathrm{an}} \gg \alpha^2 H_d$): progressive and reversible transitions are expected between the critical currents

$$j_{\mathrm{start}}^{\mathrm{P}\to\mathrm{AP}} = j_{\mathrm{end}}^{\mathrm{AP}\to\mathrm{P}} = -\frac{\alpha\gamma_0}{G_{\mathrm{P}}}\left(|H_{\mathrm{appl}}| + H_{\mathrm{an}} + \frac{H_d}{2}\right),$$

$$j_{\mathrm{end}}^{\mathrm{P}\to\mathrm{AP}} = j_{\mathrm{start}}^{\mathrm{AP}\to\mathrm{P}} = -\frac{\gamma_0}{G^{\mathrm{AP}}}[(|H_{\mathrm{appl}}| - H_{\mathrm{an}})(H_{\mathrm{appl}} - H_{\mathrm{an}} + H_d)]^{1/2}. \qquad \text{(B2)}$$

Case (b), *regime A* ($H_{\mathrm{appl}} < 0, H_{\mathrm{an}} - |H_{\mathrm{appl}}| \gg \alpha^2 H_d$): direct and irreversible transitions are expected at

$$j_c^{\mathrm{P}\to\mathrm{AP}} = -\frac{\alpha\gamma_0}{G^{\mathrm{P}}}\left(H_{\mathrm{appl}} + H_{\mathrm{an}} + \frac{H_d}{2}\right),$$

$$j_c^{\mathrm{AP}\to\mathrm{P}} = +\frac{\alpha\gamma_0}{G^{\mathrm{AP}}}\left(-H_{\mathrm{appl}} + H_{\mathrm{an}} + \frac{H_d}{2}\right). \qquad \text{(B3)}$$

Case (b), *regime B* ($H_{\mathrm{appl}} < 0, |H_{\mathrm{appl}}| - H_{\mathrm{an}} \gg \alpha^2 H_d$): progressive and reversible transitions are expected between the critical currents

$$j_{\mathrm{start}}^{\mathrm{P}\to\mathrm{AP}} = j_{\mathrm{end}}^{\mathrm{AP}\to\mathrm{P}} = +\frac{\gamma_0}{G^{\mathrm{P}}}[(|H_{\mathrm{appl}}| - H_{\mathrm{an}})(|H_{\mathrm{appl}}| - H_{\mathrm{an}} + H_d)]^{1/2},$$

$$j_c^{\mathrm{AP}\to\mathrm{P}} = +\frac{\alpha\gamma_0}{G^{\mathrm{AP}}}\left(-H_{\mathrm{appl}} + H_{\mathrm{an}} + \frac{H_d}{2}\right). \qquad \text{(B4)}$$

*On leave from the Department of Physics, Faculty of Science, HR-10000 Zagreb, Croatia.

[1] J. Slonczewski, J. Magn. Magn. Mater. **159**, 1 (1996).

[2] L. Berger, Phys. Rev. B **54**, 9353 (1996); J. Appl. Phys. **81**, 4880 (1997); Phys. Rev. B **59**, 11 465 (1999); J. Appl. Phys. **89**, 5521 (2001); **91**, 6795 (2002).

[3] M. Tsoi, A. G. M. Jansen, J. Bass, W. C. Chiang, M. Seck, V. Tsoi, and P. Wyder, Phys. Rev. Lett. **80**, 4281 (1998).

[4] J. E. Wegrowe, D. Kelly, Ph. Guitienne, Y. Jaccard, and J-Ph. Ansermet, Europhys. Lett. **45**, 626 (1999).

[5] J. E. Wegrowe, J. Appl. Phys. **89**, 7127 (2001).

[6] J. Z. Sun, J. Magn. Magn. Mater. **202**, 157 (1999).

[7] J. A. Katine, F. J. Albert, R. A. Buhrman, E. B. Myers, and D. C. Ralph, Phys. Rev. Lett. **84**, 3149 (2000).

[8] E. B. Myers, D. C. Ralph, J. A. Katine, R. N. Louie, and R. A. Buhrman, Science **285**, 867 (2000).

[9] J. Grollier, V. Cros, A. Hamzic, J. M. George, H. Jaffrès, A. Fert, G. Faini, J. Ben Youssef, and H. Le Gall, Appl. Phys. Lett. **78**, 3663 (2001).

[10] F. J. Albert, J. A. Katine, R. A. Buhrman, and D. C. Ralph, Appl. Phys. Lett. **77**, 3809 (2000).

[11] J. Z. Sun, D. J. Monsma, D. W. Abraham, M. J. Rooks, and R. H. Koch, Appl. Phys. Lett. **81**, 2202 (2002).

[12] J. Grollier, D. Lacour, V. Cros, A. Hamzic, A. Vaurès, A. Fert, D. Adam, and G. Faini, J. Appl. Phys. **92**, 4825 (2002).

[13] X. Waintal, E. B. Myers, P. W. Brouwer, and D. C. Ralph, Phys. Rev. B **62**, 12 317 (2000).

[14] Ya. B. Bazaliy, B. A. Jones, and S. C. Zhang, Phys. Rev. B **57**, R3213 (1998); J. Appl. Phys. **89**, 6793 (2001).

[15] M. D. Stiles and A. Zangwill, Phys. Rev. B **66**, 014407 (2002); J. Appl. Phys. **91**, 6812 (2002).

[16] J. C. Slonczewski, J. Magn. Magn. Mater. **247**, 324 (2002).

[17] S. F. Zhang, P. M. Levy, and A. Fert, Phys. Rev. Lett. **88**, 236601 (2002).

[18] K. Xia, P. J. Kelly, G. E. W. Bauer, A. Brataas, and I. Turek, Phys. Rev. B **65**, 220401 (2002).

[19] A. Fert, H. Jaffres, J. Grollier, and V. Cros (unpublished).

[20] K. Heide, P. E. Zilberman, and R. J. Elliott, Phys. Rev. B **63**, 064424 (2001); C. Heide, Phys. Rev. Lett. **87**, 197201 (2001); C. Heide, Phys. Rev. B **65**, 054401 (2002).

[21] J. Z. Sun, Phys. Rev. B **62**, 570 (2000).

[22] J. Miltat, G. Albuquerque, A. Thiaville, and C. Vouille, J. Appl. Phys. **89**, 6982 (2001); Z. Li and S. Zhang, cond-mat/0302337 (unpublished); cond-mat/0302339 (unpublished).

[23] F. Schreiber, J. Pfaum, and J. Pelzl, Solid State Commun. **93**, 965 (1995).

[24] J. Bass and W. P. Pratt Jr., J. Magn. Magn. Mater. **200**, 274 (1999).

[25] A. Fert and L. Piraux, J. Magn. Magn. Mater. **200**, 338 (1999).

[26] D. X. Chen, E. Pardo, and A. Sanchez, IEEE Trans. Magn. **38**, 742 (2002).